

SUMMARY OF STATIC LOAD TEST OF THE MOD-0 BLADE

Dean R. Miller

National Aeronautics and Space Administration
Lewis Research Center
Cleveland, Ohio 44135

ABSTRACT

A static load test was performed on the spare Mod-0 windturbine blade to define load transfer at the root end of the blade, and to validate stress analysis of this particular type of blade construction (frame and stringer).

Analysis of the load transfer from the airfoil skin to the shank tube predicted a step change in spanwise stress in the airfoil skin at station 81.5 inches (STA 81.5). For flatwise bending a 40% reduction in spanwise stress was predicted, and for edgewise bending a 6% reduction. Experimental results verified the 40% reduction for flatwise bending, but indicated about a 30% reduction for edgewise bending.

The agreement between experimental and predicted results was quite good. For flatwise bending, the predictions were about 11% low between STA 81.5 and STA 120. Results for edgewise bending fell between predictions for the trailing edge skins cross-sectional area being 100% effective and 0% effective in carrying bending moment. The trailing edge skins appeared to be about 50% effective.

INTRODUCTION

A static load test was performed on the spare Mod-0 windturbine blade. The purpose of the test was twofold: (1) to evaluate load transfer at the root end of the blade between the airfoil skin and shank tube, and (2) to validate the stress analysis of this frame and stringer metal blade.

ANALYSIS OF LOAD TRANSFER

At the root end of the blade, bending moment is transferred to the shank tube by the action of a "shear couple" between two D-SPAR ribs (at stations 48 and 81.5 inches), and by means of 24 bolts connecting the shank tube to the D-SPAR rib at STA 81.5. Figure 1-A shows a cutaway view of the D-SPAR between STA 48 and STA 81.5. The rib at STA 81.5 has 24 bolts oriented radially around the shank tube.

A freebody diagram of the idealized airfoil is shown in Figure 1-B. The loads on the airfoil create a bending moment M_0 . To maintain static equilibrium, the shank tube provides a reaction to this moment by applying a shear force "V" at each structural rib, thereby creating a "shear couple." The bolts in the rib at STA 81.5 also resist " M_0 ," by applying a redundant moment " M_1 " to the airfoil. The term redundant is used because these bolts were primarily

intended to resist centrifugal loads on the airfoil, while the "shear couple" was assumed to transfer all the bending moment. However, a review of the above assumption, led to the suggestion that the bolts might actually be transferring a significant portion of the moment " M_0 ." As such, the redundant moment " M_1 " was predicted to cause a step change in spanwise airfoil stress at STA 81.5. A maximum reduction in stress of 39% was predicted for flatwise bending, and a maximum of 6% for edgewise bending.

TEST APPARATUS

Figure 2 is a photo of the overall test set up. The blade was bolted to a test support stand. Loads were applied vertically (up and down) for four 90° orientations of the blade. These four orientations provided data for tension and compression of both the high pressure surface and the leading edge.

The blade was instrumented with strain gages to sense only spanwise strain. As shown in Figure 3, the gages were clustered about station 81.5 inches (STA 81.5) on the high pressure surface and on the leading edge.

TEST RESULTS

The results of the test are shown in Figures 4 and 5. In both figures, the ratio " σ/M " is plotted as a function of spanwise blade station. The ratio " σ/M " is the ratio of measured spanwise stress to the total bending moment (be that flatwise or edgewise). It is used because it provides a means of comparing stress levels at various spanwise locations along the blade, but still accounting for the different local cross-sectional properties.

Stress in the high pressure surface of the blade due to flatwise bending is shown in Figure 4. The solid dark line indicates the prediction, while the dashed line represents the experimental results. Locations of the D-SPAR ribs are shown by the "speckled" regions centered about STA 48 and STA 81.5.

As predicted there was about a 40% drop in airfoil stress across the rib at STA 81.5. Between STA 48 and STA 81.5, the experimental results agreed quite closely with the predicted behavior. Outboard of STA 81.5, the results were about 11% higher than the predictions. The little peak at STA 85.5 was attributed to some local bending effects of the airfoil skin over the D-SPAR rib at STA 81.5.

The leading edge stress due to edgewise bending are shown in Figure 5. Again, the solid dark lines indicate predicted results, while the dashed lines represent experimental results. There are two predicted lines: one which assumes none of the cross-sectional area of the trailing edge skin is effective in carrying bending moment (0%), and one which assumes all of the cross-sectional area is effective (100%).

The experimental data indicated about a 30% reduction in airfoil stress across the rib at STA 81.5. This was significantly more (24%) than predicted. For edgewise bending then, the shank tube bolts are actually carrying approximately 1/3 of the total bending moment.

In general, the data fell between the two predicted lines for 0% and 100% effective trailing edge skins. Attributing the peak at STA 87.5 to local bending of the airfoil over the D-SPAR rib, the data seem to indicate about a 50% effective trailing edge. Information from a previous static load test seemed to suggest that 50% was a good value for trailing edge effectiveness.

CONCLUSIONS

With regard to evaluating load transfer at the root end of the blade:

1. 40% of the flatwise bending moment in the airfoil was transferred to the shank tube thru the shank tube bolts.
2. 30% of the edgewise bending moment in the airfoil was transferred to the shank tube thru the shank tube bolts.

In general, the experimental results validated our predictions. The results indicated:

1. Spanwise stress in the airfoil due to flatwise bending moment was 11% above the predictions for stations beyond 81.5.
2. The cross-sectional area of the trailing edge skins was 50% effective in carrying edgewise bending moment.

REFERENCES

1. Timoshenko, S.; and Goodier, J. N.: Theory of Elasticity, 2nd Edition, McGraw Hill, 1951.
2. Cherritt, A. W.; and Gaidelis, J. A.: 100-kW Metal Windturbine Blade Basic Data, Loads and Stress Analysis, Report No. LR 27153, Lockheed California Company, 6-17-75.
3. Spera, D. A.: Structural Analysis of Wind Turbine Rotors for NSF-NASA Mod-0 Wind Power System, NASA TMX-3198, March 1975.

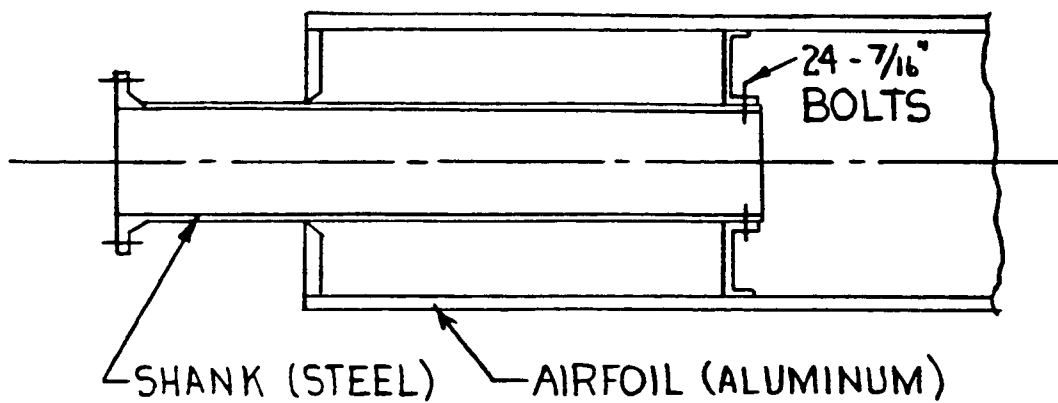
DISCUSSION

- Q. The outboard rib which was not designed to carry diaphragming type loads was found to be carrying 40% of the blade bending load as a diaphragming load. Doesn't this present a static or fatigue stress problem?
- A. Fortunately, no. The rib was conservatively designed to carry a very high shear load and as a result, rib stresses remained below skin stresses even with the additional diaphragm load.
- Q. Did you make any shear flow calculations?
- A. Shear flow calculations were performed by the blade manufacturer and are contained in reference 2.

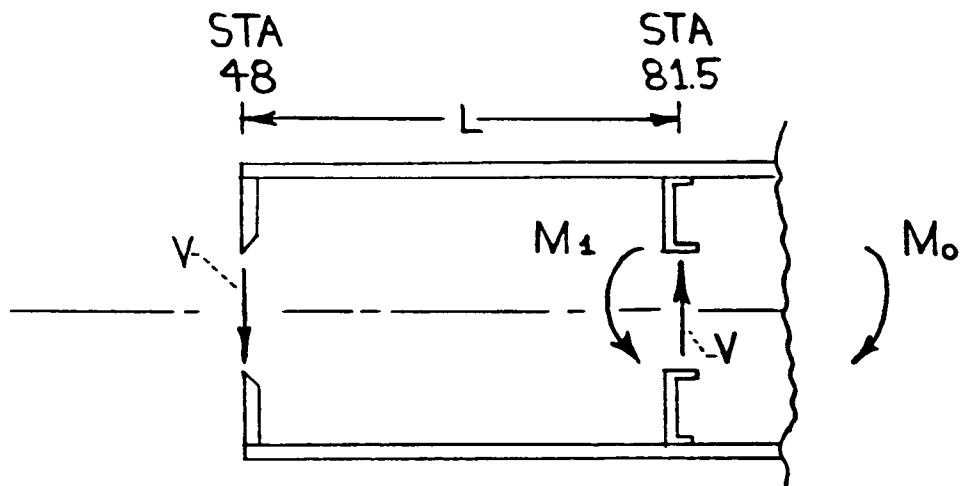
- Q. Did you assess the strain at the trailing edge (roughly 50% span) to check for buckling?
- A. Buckling was of the local panel type, rather than overall buckling of the trailing edge itself, and was observed both visually and through strain gage data.

COMMENT:

With regard to the effectiveness of trailing edge skins, an exact analysis of skin load transfer for airfoil shapes at skin endings is available. It was performed by Dr. Biot.



(a) Cutaway view of idealized blade.



$V \equiv$ SHEAR FORCE

$M_o \equiv$ BENDING MOMENT DUE TO BLADE LOADS

$M_1 \equiv$ REDUNDANT MOMENT DUE TO SHANK BOLTS

(b) Free-body diagram of airfoil.

Figure 1. - Root end of Mod-0 wind turbine blade.

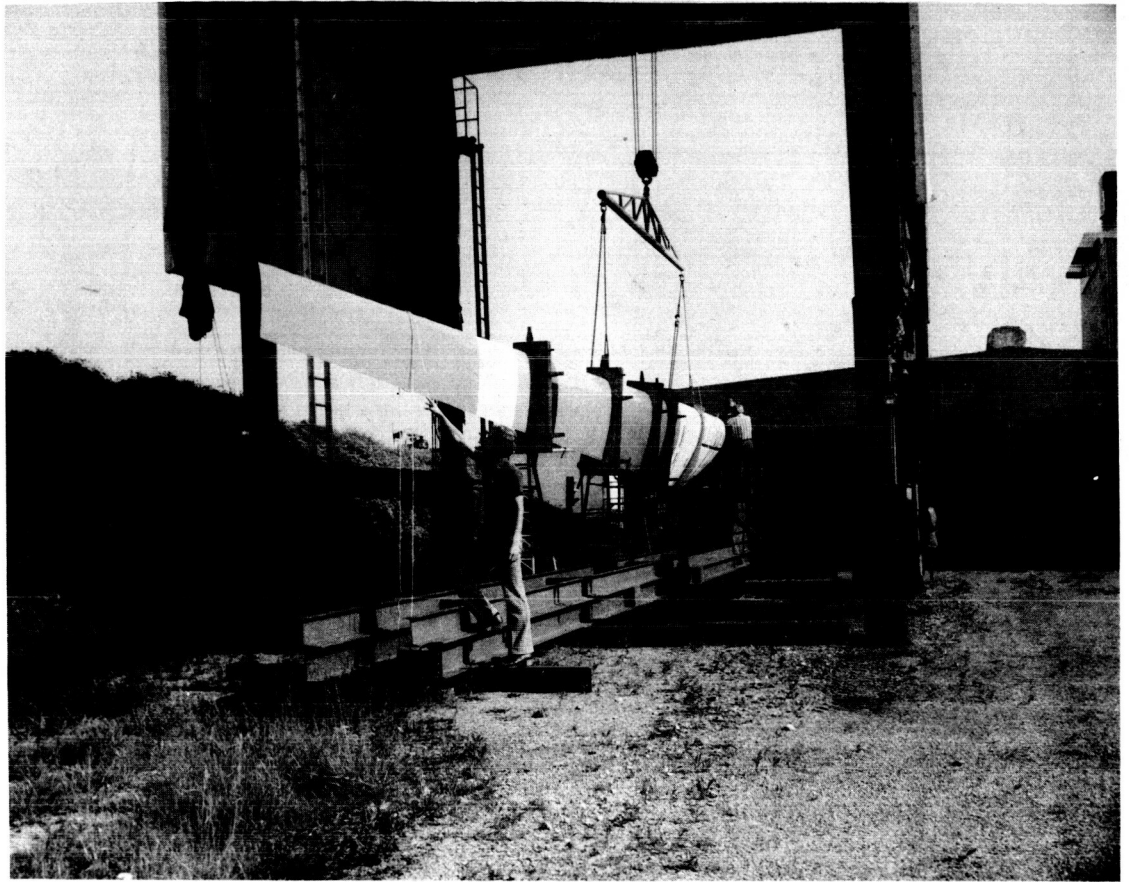


Figure 2. - Test setup for static load test of Mod-0 blade.

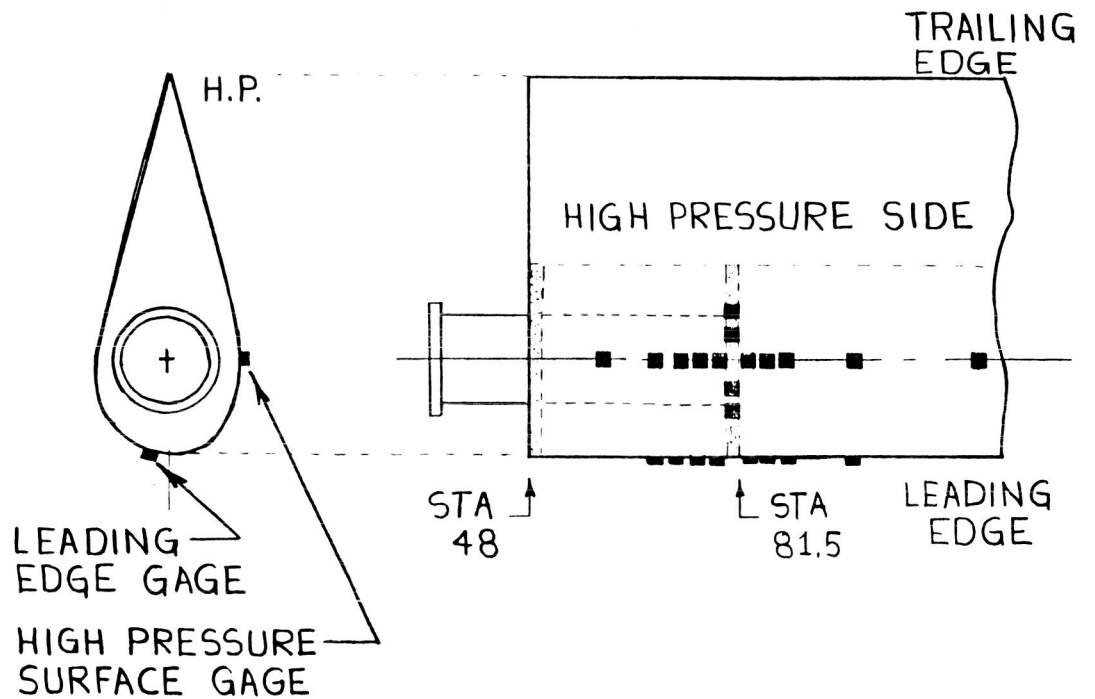
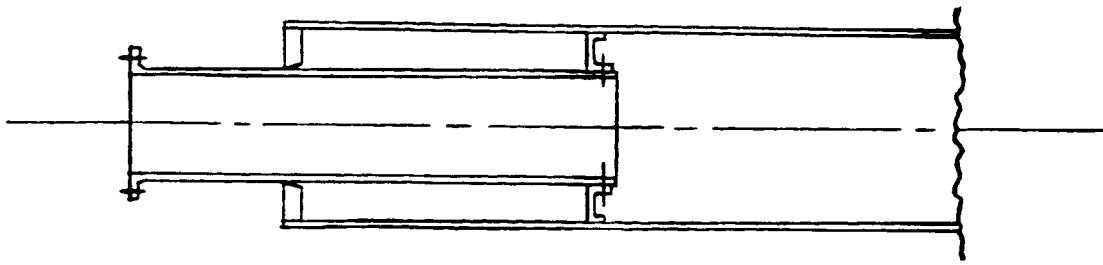


Figure 3. - Strain-gage location on Mod-0 blade for static load test.



RATIO OF SPANWISE STRESS
TO APPLIED FLATWISE MOMENT

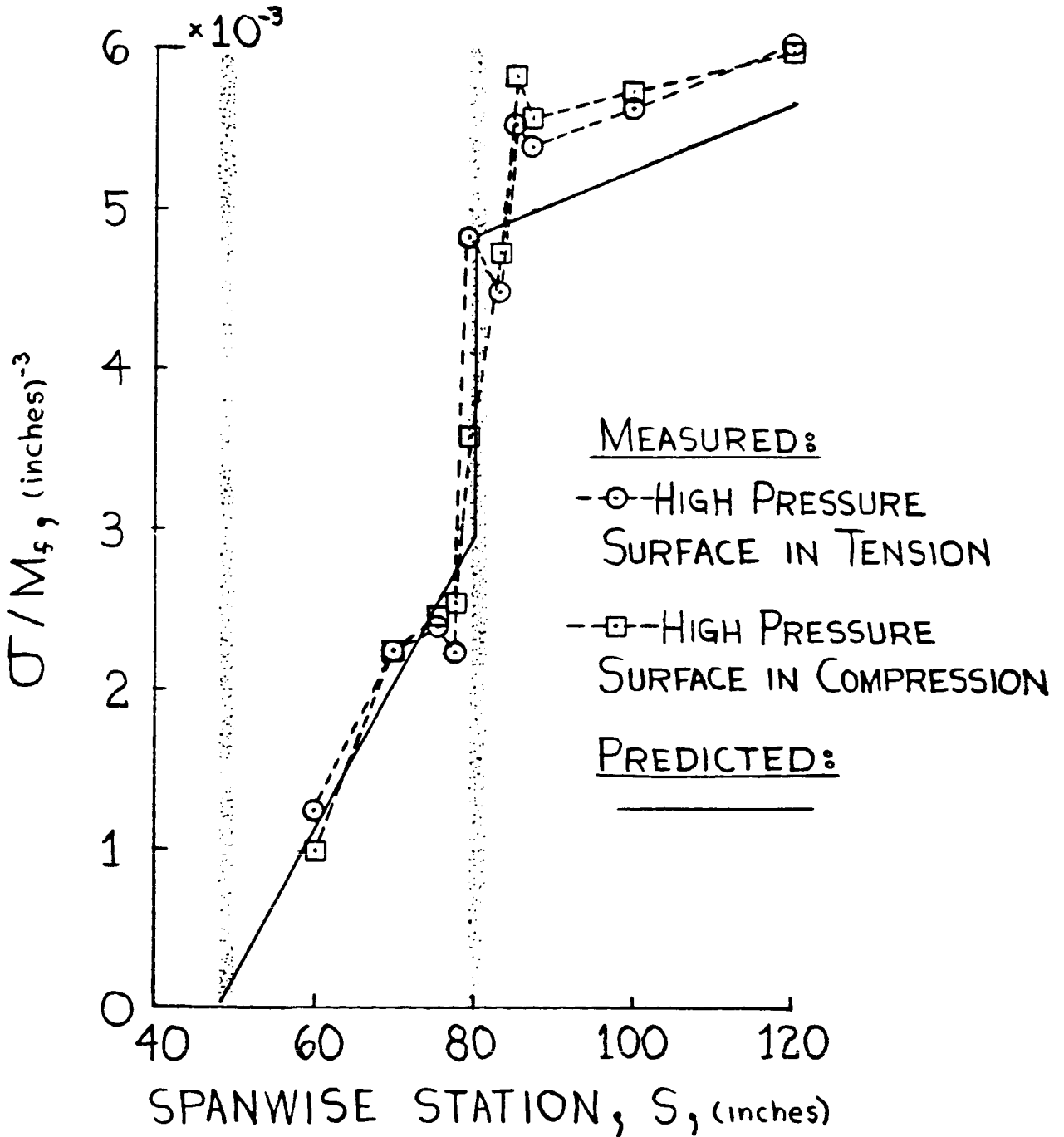


Figure 4. - High-pressure surface stress.

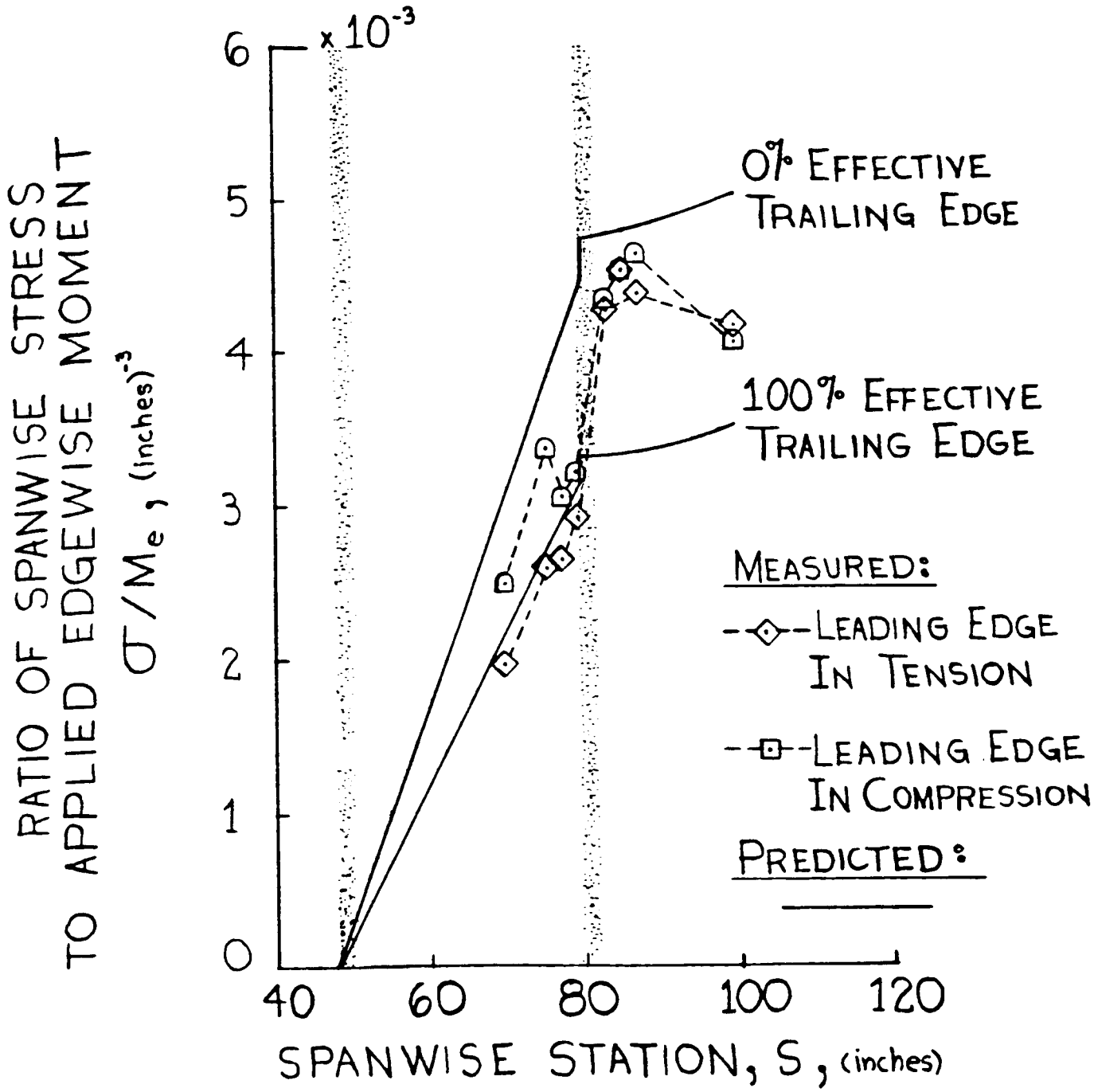
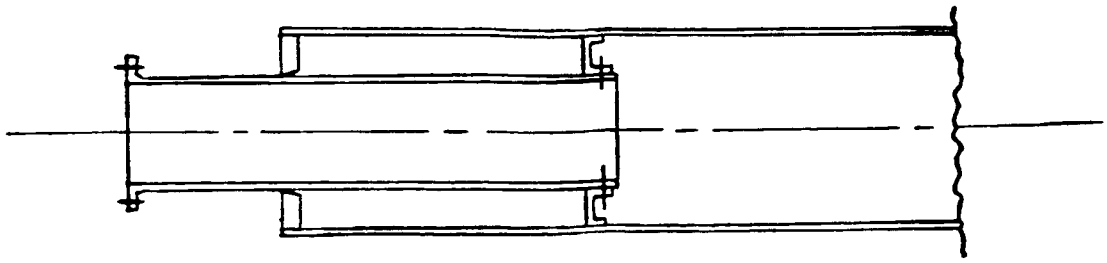


Figure 5. - Leading-edge stress.